Meteoritics & Planetary Science 38, Nr 9, 1299–1317 (2003)
Abstract available online at http://meteoritics.org

The suevite of drill hole Yucatàn 6 in the Chicxulub impact crater

Philippe CLAEYS,[1*] Sabine HEUSCHKEL,[2] Elena LOUNEJEVA-BATURINA,[3]
Gerardo SANCHEZ-RUBIO,[3] and Dieter STÖFFLER[4]

[1]Department of Geology, Vrije Universiteit Brussel, Pleinlaan 2, B-1050 Brussels, Belgium
[2]ZERIN (Center for Ries Crater and Impact Research), Vordere Gerbergasse 3, 86720 Nördlingen, Germany
[3]Institute of Geology (UNAM), Ciudad Universitaria, Apartado Postal 70–296, 04510 México, D.F., Mexico
[4]Institut für Mineralogie, Museum für Naturkunde, Humboldt-Universität zu Berlin, Invalidenstrasse 43, 10099 Berlin, Germany
*Corresponding author. E-mail: phclaeys@vub.ac.be

(Received 20 December 2002; revision accepted 7 August 2003)

Abstract–The suevite breccia of the Chicxulub impact crater, Yucatàn, Mexico, is more variable and complex in terms of composition and stratigraphy than suevites observed at other craters. Detailed studies (microscope, electron microprobe, SEM, XRF) have been carried out on a noncontinuous set of samples from the drill hole Yucatàn 6 (Y6) located 50 km SW from the center of the impact structure. Three subunits can be distinguished in the suevite: the upper unit is a fine-grained carbonate-rich suevite breccia with few shocked basement clasts, mostly altered melt fragments, and formerly melted carbonate material; the middle suevite is a coarse-grained suevite with shocked basement clasts and altered silicate melt fragments; the lower suevite unit is composed of shocked basement and melt fragments and large evaporite clasts. The matrix of the suevite is not clastic but recrystallized and composed mainly of feldspar and pyroxene. The composition of the upper members of the suevite is dominated by the sedimentary cover of the Yucatàn target rock. With depth in well Y6, the amount of carbonate decreases and the proportion of evaporite and silicate basement rocks increases significantly. Even at the thin section scale, melt phases of different chemistry can be identified, showing that no widespread homogenization of the melt took place. The melt compositions also reflect the heterogeneity of the deep Yucatàn basement. Calcite with characteristic feathery texture indicates the existence of formerly pure carbonate melt. The proportion of carbonate to evaporite clasts is less than 5:1, except in the lower suevite where large evaporite clasts are present. This proportion constrains the amount of CO_2 and SO_X released by the impact event.

INTRODUCTION

The ~200 km diameter Chicxulub impact crater on the Yucatàn Peninsula is most likely responsible of the Cretaceous-Tertiary (KT) boundary mass extinction. To what extent, precisely, the huge amount of energy released by the impact perturbed the global Earth system and the biosphere remains to be constrained. In the late Cretaceous, the Yucatàn Peninsula was a shallow water platform consisting of approximately 2 to 3 km of carbonates and evaporites resting on a Pan-African basement (Lopez-Ramos 1975; Krogh et al. 1993). The impact presumably injected large quantities of volatiles (CO_2, H_2O, SO_X) and dust, which were released by shock vaporization and comminution of the target rock into the atmosphere. Their accumulation in the atmosphere likely lead to a strong perturbation of the Earth's climate (Pope et al. 1994; Ivanov et al. 1996; Pope et al. 1997; Pierazzo et al. 1998; Yang and Ahrens 1998; Gupta et al. 2001). Recently, several models converged toward a calculated volume in the range of 10^{17} g of SO_X released. However, the precise quantification of the amounts of CO_2 and SO_X released from shocked carbonates and evaporites is still a matter of debate. This is because the exact proportion of carbonate and evaporite in the sediment forming the upper 3 km of the Yucatàn target rock remains difficult to estimate and because experimental data only recently began to set constrains on the mechanism and treshold pressures required for complete shock vaporization of carbonates and anhydrite (Yang and Ahrens 1998; Gupta et al. 2001; Ivanov and Deutsch 2002). The composition of the Chicxulub impactites may provide valuable information to evaluate the amount and type of material vaporized and ultimately document the effects on climate and the subsequent evolution of life.

The crater was first drilled more than 30 yr ago for exploration purposes by the Mexican oil company PEMEX (Fig. 1). Preserved fragments of the recovered drill cores were

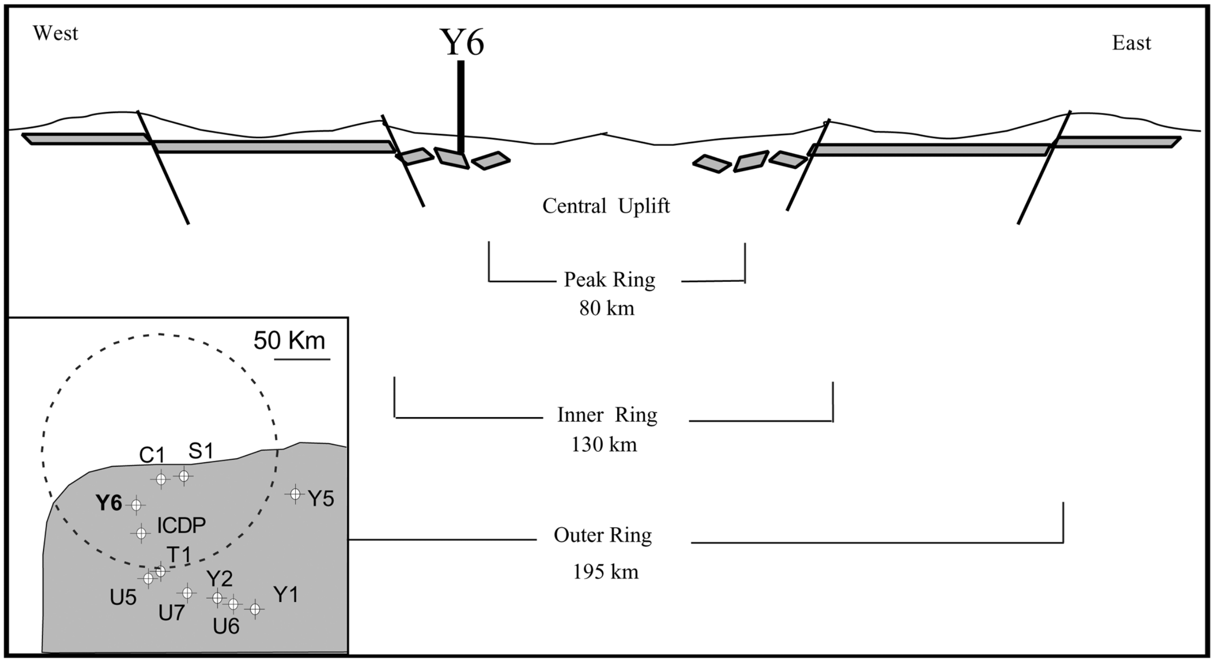

Fig. 1. Position of the Yucatàn 6 borehole on the schematic crater model of Morgan et al. (1997) and the location of the different wells drilled in the Chicxulub structure.

used to confirm the impact origin and KT boundary age of the structure (Hildebrand et al. 1991; Kring and Boynton 1992; Swisher et al. 1992). Two types of impactite lithologies were identified: suevite breccia and impact melt rock (Sharpton et al. 1992; Swisher et al. 1992; Hildebrand et al. 1993; Koeberl et al. 1994; Schuraytz et al. 1994; Sharpton et al. 1996; Warren et al. 1996). Previous studies considered the Chicxulub impact breccia from well Yucatàn 6 (Y6) as a typical suevite with abundant shocked basement fragments, glass, and deformed melt clasts (Schuraytz et al. 1994; Sharpton et al. 1996; Warren et al. 1996; Claeys et al. 1998). These studies revealed that the suevite grades from sand-sized clasts in the upper part to pebble-sized clasts downward and is comparable to that observed at other craters, for example, the Ries in southern Germany.

Closer examination of the suevite indicates that the situation is more complex. This paper presents petrological, mineralogical, and geochemical data of suevite samples from well Y6 (Fig. 1). It shows that in Y6, the Chicxulub suevite is sorted vertically in terms of composition and that it is divided into several members based on clast origin and type. The significant portion of carbonates, including melt phases, omnipresent in the upper part of the suevite is of particular interest. Hildebrand et al. (1991) had first noticed that the Chicxulub suevite contains an unusual fine-grained calcite matrix. Suevite is, by definition, an impactite with a clastic matrix and cogenetic melt inclusions (Stöffler et al. 1979; Stöffler and Grieve 1994). Although the Chicxulub Y6 suevite broadly fits this definition, the abundance of carbonate phases, both as clasts and in the matrix, and the recrystallized matrix in the deepest suevite layer render it somewhat peculiar in comparison to the silicate-dominated suevite observed at most craters. The type and origin of the various carbonate phases yield information concerning the vaporization, melting, and shock processes that affected the Yucatàn target rock.

PRE-IMPACT LITHOLOGIES OF THE YUCATÀN PLATFORM

Models indicate that the Chicxulub impact should have excavated the Yucatàn platform down to a depth of 12 to 14 km (Kring 1995). Considering the dimensions of the crater transient cavity (±100 km in diameter) (Morgan et al. 1997), a great variety of lithologies must have been sampled by the event. Based on the Lopez-Ramos (1975) study of drilling results over Yucatàn, the basement underneath the Peninsula is of Pan-African age (±550 Ma; Krogh et al. 1993) and consists of quartz chlorite schist, quartzite, granites, and volcanic rocks such as rhyolites. Clastic red beds, siltstones, sandstones, and silty dolomite of either Triassic or Jurassic to early Cretaceous ages occur above the crystalline basement. The lateral extend and thickness of these units are poorly constrained. The overlying Cretaceous succession is composed of a 2 to 3 km thick sequence of shallow water limestones and dolomite interbedded with anhydrite. The exact proportion of evaporite to carbonate is not known. Estimates of the evaporite content based on drill cores, logs, and well cuttings range from 23% to almost 60% (Lopez-Ramos 1975; Ward et al. 1995). The stratigraphic sequence of the Yucatàn target rock involved in the Chicxulub impact is lithologically complex; this study shows that the suevite sequence reflects the heterogeneous stratigraphy and composition of the target sequence.

SAMPLES AND ANALYTICAL TECHNIQUES

The focus of this study is the characterization of the Chicxulub suevite from well Yucatàn 6 (Y6). If projected on the offshore BIRPS seismic line (Morgan et al. 1997), the Y6 well lies slightly outside of the peak ring area, less than 50 km SW from the center of the Chicxulub impact structure (Fig. 1). Fourteen samples of suevite from well Y6 were studied, first macroscopically, then by optical and electron scanning microscopy. The composition and abundance of the different types of clasts and matrix were quantified as was the degree of shock metamorphism in quartz and feldspar. Extensive semi-quantitative and quantitative analyses were carried out with scanning electron microscope (JEOL JSM 6300, EDX; 20 kV, 7 nA) and electron microprobe (JEOL JXA 8800; 15 kV, 5 nA; beam diameter: 1–10 microns) at the Museum für Naturkunde in Berlin and at the UNAM in Mexico City. Depending on availability, between 2 and 10 g of sample material were pulverized and homogenized. The glass beads of the bulk suevite samples were prepared (0.6 g sample + 3.6 g flux) and analyzed for major and minor element composition by X-ray fluorescence on an automated SIEMENS SRS 3000. The CO_2 and H_2O contents were determined using a Rosemount CWA 5003 spectrometer.

One must remember that this study is based on a noncontinuous set of just 14, smaller than fist-size samples collected from fragments of the remaining core drilled outside the peak ring of the Chicxulub crater. The total thickness of the suevite in this Y6 well is estimated to be approximately 250 m (Sharpton et al. 1996). Based on the available core fragments, the thickness of the different units described here is, thus, difficult to determine. The conclusions drawn here must be viewed as preliminary; they may apply only to the peak ring area, providing a small window on a large crater apparently characterized by rather complex and variable impactite lithologies.

PETROGRAPHY OF THE SUEVITES

The Chicxulub suevite is more complex than previously assumed and differs from a typical silicate-rich suevite as described at the Ries-type locality and at other craters (Stöffler et al. 1979). The observed Chicxulub suevite is clearly stratified in terms of composition, grain size, type of matrix, concentration of melt material, and distribution of shocked lithic and mineral clasts. Three distinct types of suevite breccia can be identified in the available samples. They are described below from top to bottom as they appear in the Y6 well (Fig. 2).

1. An upper suevite (or carbonate-rich suevite). Small densely packed carbonate clasts clearly dominate over crystalline basement fragments. The clasts are embedded in a porous, 10 micron-size matrix composed mainly of calcite, feldspar, and quartz (Nucleo [N] 13: 1100–1103 mbsl; samples: Y6 N13–3; Y6 N13–4, Y6 N13–5, Y6 N13–9).
2. A middle suevite (or clast-rich suevite). The silicate basement clasts and altered silicate melt fragments increase in proportion with depth. The clasts are suspended in a more compacted and much less porous matrix. (N14: 1208–1211 mbsl; samples: Y6 N14–1, Y6 N14–4, Y6 N14–5a/5b, Y6 N14–6, Y6 N14–10, Y6 N14–11a/11b, Y6 N14–15, Y6 N14–x1/x2).
3. A lower suevite (or thermometamorphic suevite). This is composed of basement and evaporite clasts and abundant silicate melt fragments. The matrix is completely recrystallized and consists of euhedral feldspar and pyroxene grains. (N15: 1253–1256 mbsl; sample: Y6 N15).

Upper Suevite (Carbonate-Rich Suevite)

The upper part of the microbreccia is mainly composed of small angular to subangular carbonate clasts (locally >75%) and a few feldspar and quartz fragments (Fig. 3). Most clasts range in size between 0.5 and 1 mm. Clasts composed of clay minerals are also present. They have elongated shapes and are often molded or wrapped around other clasts, especially carbonates. They also occur as 400–600 μm-sized isolated shards. A few amphibole minerals with a size of 300 μm are randomly distributed; EDX analyses seem to indicate a gedrite mineralogy. Many of the quartz grains are recrystallized and only one clearly contains shock-induced planar deformation features (PDFs). As a whole, solid fragments of the deep Yucatàn silicate basement are rare; they form approximately 10% of the clasts in this unit that is essentially dominated by carbonates and melt phases (±15%). Anhydrite clasts are also rare, but anhydrite occurs as a secondary pore filling phase. The matrix (grain size 10–15 μm) contains small crystals of calcite (25%), plagioclase (30%), quartz (30%), K-feldspar (10%), and amphibole (5%) (Fig. 4).

Several types of carbonate fragments can be identified. The most common are rounded clasts of dark micrite without discernible internal structure. They represent approximately 60% of the carbonate clasts and are usually about a mm in size. They resemble intraclasts, mud pebbles, and aggregated grains, similar to those forming today in shallow water environments of the Bahamas banks, for example (Flügel 1982). Fossil fragments can be identified in some of the largest micrite grains (Fig. 3a), in particular, upper Cretaceous foraminifera such as orbitoids as well as algae, bivalve, gastropod, and sponge fragments. The characteristic cellular-

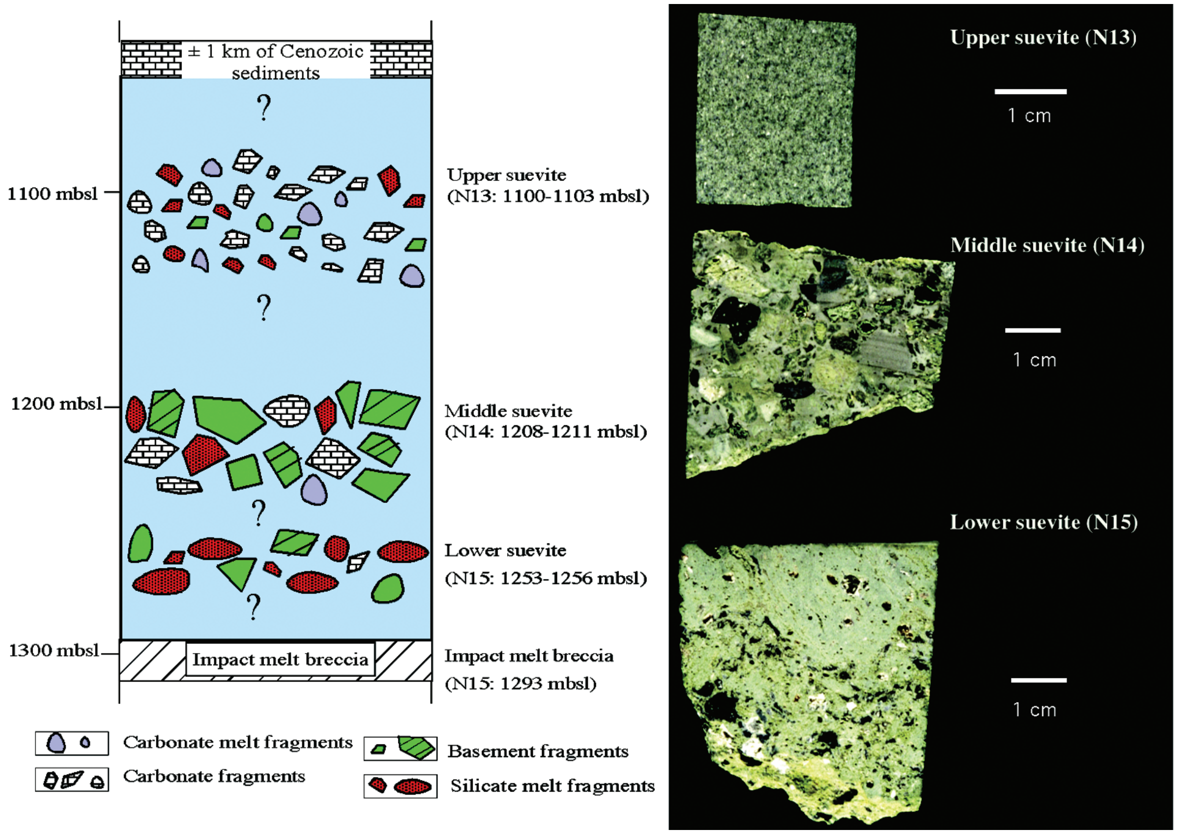

Fig. 2. Schematic lithostratigraphic section of the noncontinuous set of samples studied, with macroscopic photos of the 3 different types of suevite identified in well Y6 on the right. The characteristic variations in clast size, type, and composition between the 3 units is clearly visible on the photos. The depths given on the left side of the section are only indicative, the exact thickness of the units is not known. The sample depth as written on the remaing core fragments is given on the right side of the section.

prismatic structure of rudists can also be recognized in several of the largest grains. The fauna represents facies typical of a shallow water carbonate platform such as the Yucatàn Peninsula at the time of impact. All identified fossil fragments are of upper Cretaceous age. This unit was previously interpreted as upper Cretaceous stratified limestone (Lopez-Ramos 1975) and was later used by some authors as evidence to advocate a pre-KT boundary age for the Chicxulub crater (Ward 1996). As clearly pointed out by Sharpton et al. (1996), this unit is an integral part of the Chicxulub impactite as attested by the presence of abundant melt fragments and sporadic shocked grains. It cannot be used as a biostratigraphic unit.

Other, more unusual carbonate clasts are composed of single, often angular-shaped sparry calcite crystals (Fig. 3a). They form about 25% of all carbonate clasts. These crystals are clear and almost free of impurities or inclusions. They resemble diagenetic cement, but closer examination and, in particular, their association with other clasts and the matrix indicate that they are not a secondary pore cementing phase. Comparable calcite crystals occur in the impact ejecta bed at the Mimbral KT boundary site (Claeys et al. 1996).

The most unusual carbonate clasts are elongated calcite grains with a diagnostic feathery or spinifex texture (Jones et al. 2000). These grains reach between 2 and 3 mm in size. Under cathodoluminescence, every carbonate phase luminesces except for this feathery calcite (Heuschkel et al. 1998). The feathery texture is formed of radiating to almost parallel aggregates of numerous fine-scale, 100–200 µm size elongated calcite crystals. Under crossed polars, they have a zoned or irregular extinction. These larger grains are irregularly distributed and most commonly occur isolated from other clasts in the fine-grained matrix. The feathery calcite observed in the upper Chicxulub suevite strongly resembles the branching or comb-layered textures occurring in the carbonatite dikes from the Kaiserstuhl volcanic intrusions in Germany (Katz and Keller 1981). Similar occurrences are also reported from experimentally rapidly quenched carbonate melt (Wyllie 1989). Based on these similarities, Jones et al. (2000) have interpreted the largest (>~1 mm) feathery crystals (Fig. 5) as formerly molten carbonate phases. Closer examination revealed that many of the finer size calcite crystals also display this feathery calcite texture (Fig. 5). These grains range in size between 30 and 300 microns and can be difficult to distinguish from the calcite matrix. Their identification shows that molten material represented a

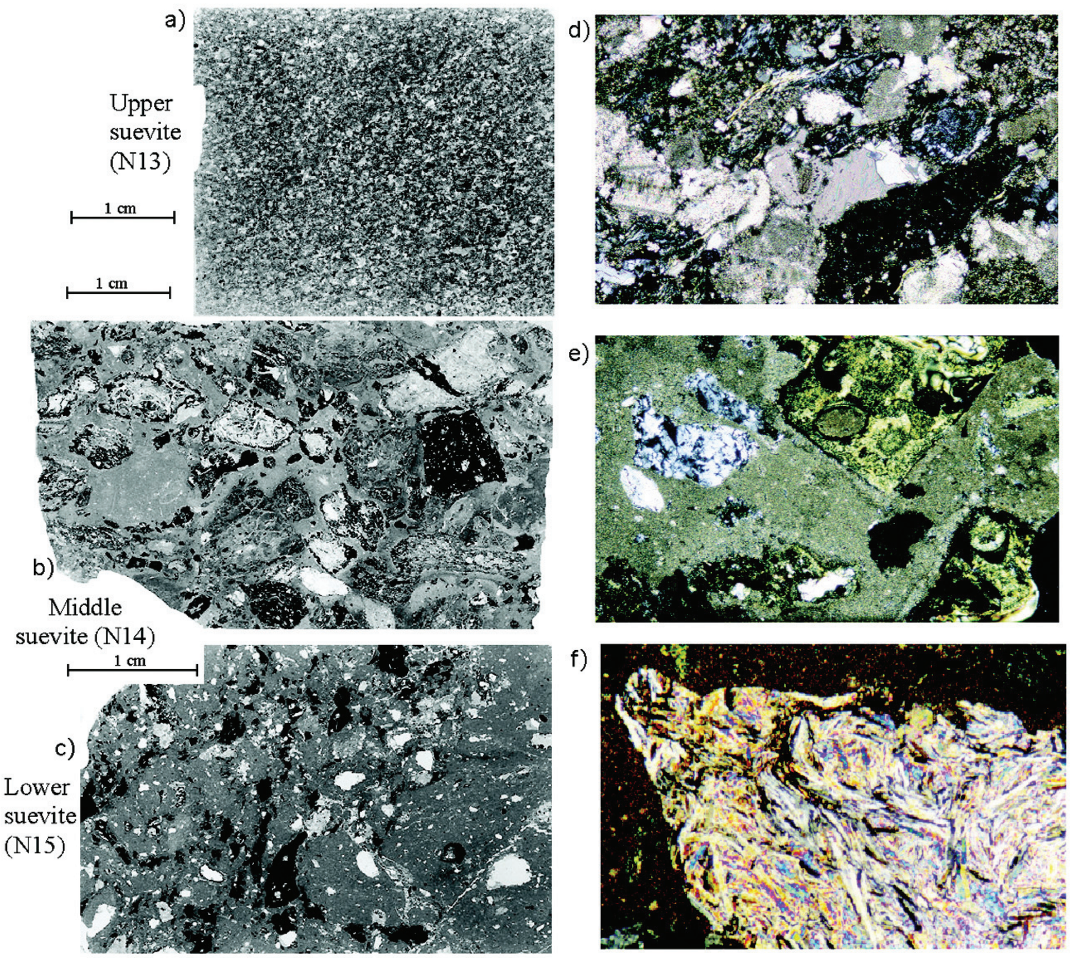

Fig. 3. On the left side, thin section photos showing: a) the fine texture of the upper suevite; b) the melt (black), carbonate (grey), and basement clasts found in the middle suevite; c) the lower suevite with melt clast (dark) and quartz or feldspar clasts (white/grey). On the right: d) clast and groundmass distribution in the upper suevite with melt fragment (dark), sparry calcite (pinkish), micritic carbonate, and fossil remnants (left side) (crossed nicols; field of view: 6 mm); e) characteristic overview of clasts in the middle suevite; carbonate clast with fossils (upper right), dark melt fragments, oval anhydrite clast (white fragment in lower part, mid-section), and basement clasts in a fine-grained groundmass (crossed nicols; length of picture: 6 mm); f) one of the large clasts of anhydrite found in the lower suevite surrounded by the annealed matrix. A small rounded silicate melt clast is also visible in the upper right corner of the picture (crossed nicols; length of picture: 2.5 mm).

significant component (up to 15%) of all the carbonate phases produced by the impact in this zone of the crater.

The almost isotropic, commonly elongated fragments or shards of clay minerals (Table 1) are probably altered glass or melt particles. These grains are often altered, however small (~20 μm), but pristine glass phases (Table 2) can still be identified in several grains. In the suevite, SEM observation shows that the preserved glass occurs in the center of the particles and that it grades toward palagonite-like material at the rim. Micron-size needles and small spherules of carbonate material also occur in these fragments. Their elongated morphology, more or less aligned parallel with the flow structure still noticeable in the altered glass, and clean contacts with the surrounding altered glass supports a primary origin rather than a secondary filling phase. They ressemble the carbonate globules identified by Graup (1999) in melt fragments from the Ries crater suevite.

Macroscopic observations of the available samples seem to indicate that this carbonate-dominated suevite is layered. The layering appears to be composed of alternating melt-rich (both silicate and carbonate) and melt-poor horizons, usually around <5 mm thick. However, this observation is only based on a small (7 × 3 cm) piece of core and may not be representative of the whole unit; it will have to be confirmed by macroscopic observation on a more complete sequence of suevite from a larger piece of core.

The clastic matrix occurring between the clasts contains crystals of calcite (22%), plagioclase (16%), quartz (40%), K-feldspar (16%), and amphibole (6%) (Fig. 4). The proportion of the different components can vary significantly, even at the thin section scale. The size of the crystals varies between 5 and 20 μm. The feldspar and quartz minerals are subrounded, while the morphology of the calcite grains can be rounded or angular (Fig. 4). The amphiboles are elongated and stretched between

Table 1. Electron microprobe analyses of clay minerals aggregates (alteration products of melt particles) in the Chicxulub suevite (samples N13 and N14) showing the differences in composition in the upper and middle suevite.[a]

	Upper suevite (N13)			Middle suevite (N14)					
SiO_2	42.0	43.4	42.3	51.5	42.8	42.6	43.1	44.3	43.1
Al_2O_3	17.0	17.0	16.0	9.5	10.5	14.2	13.8	14.1	13.1
FeO	12.6	13.8	14.1	7.3	20.7	18.5	17.3	13.2	16.9
MgO	22.9	22.0	22.1	9.0	18.3	19.3	20.5	15.5	19.9
CaO	1.6	1.9	1.8	12.2	1.9	2.3	3.6	3.1	2.9
Na_2O	n.d	n.d	n.d	2.8	n.d	n.d	n.d	2.6	n.d
K_2O	n.d	n.d	n.d	1.1	n.d	n.d	1.1	0.7	n.d
Total	96.2	98.1	96.2	93.4	94.2	96.8	99.4	93.5	95.8

[a]Analytical conditions: JEOL JXA 8800; 15 kV, 5 nA; beam diameter: 10 microns.

Table 2. Electron microprobe analyses of melt fragments in the Chicxulub suevite with high Na_2O and K_2O contents in the upper suevite (N13) and enrichment in FeO, MgO, and CaO, as well as the depletion in K_2O in the middle and lower suevite.[a]

	Upper suevite (N13)				Middle suevite (N14)				Lower suevite (N15)			
	Avg	S.d.	Min	Max	Avg	S.d.	Min	Max	Avg	S.d.	Min	Max
SiO_2	65.2	2.03	62.1	68.6	64.7	1.02	63.9	66.0	62.3	1.39	60.7	64.0
Al_2O_3	20.3	2.37	17.9	25.6	18.1	0.50	17.7	18.8	16.6	0.74	15.8	17.4
TiO_2	1.8	0.60	1.4	2.5	1.2	0.01	1.2	1.2	n.d	–	–	–
FeO	0.2	0.09	0.1	0.9	3.9	0.50	3.5	4.6	5.5	0.64	4.7	6.0
MgO	0.1	0.07	0.0	0.7	2.9	0.24	2.7	3.2	2.0	0.40	1.5	2.4
CaO	1.3	2.01	0.2	3.7	2.7	0.17	2.6	3.0	3.2	0.66	2.5	3.9
Na_2O	3.7	2.09	1.5	7.6	6.5	0.59	6.0	7.3	4.6	1.01	3.2	5.4
K_2O	10.1	3.87	2.3	14.7	1.6	0.83	0.6	2.6	5.6	1.53	4.1	7.6
Total	99.2				100.1				98.7			

[a]Analytical conditions: 15 kV, current 5 nA; beam diameter 1 micron, averages are based on 35 analyses.

the other minerals. No clear size or morphology sorting is observed, however, locally at a small scale, some bands appear to be richer in calcite or feldspar. 30 to 50 μm areas entirely composed of calcite also exist. The carbonates and feldspars are often in point or line contacts. Local grain penetration and crystal displaced by others can be seen as evidence for a slight mechanical and diagenetic compaction of the matrix most likely due to the loading effect of the overlying units. The matrix porosity varies greatly from place to place, and the morphology of the pore space is highly irregular (Fig. 4). The original porosity is difficult to estimate as many of the pore spaces are now partially filled by clay minerals and/or zeolite or evaporite phases. Locally, the grains are packed with less than 20% porosity; more commonly, large gaps occur in the matrix (Fig. 4). Other areas comprise aggregates of secondary zeolites and clay minerals. These perhaps indicate that another matrix component existed at the time of deposition. We find it difficult to speculate if this now vanished component was evaporitic or was another melt phase that is now altered to clay and/or zeolites aggregates.

The upper suevite varies greatly in bulk rock composition (Table 3; Fig. 6); SiO_2 content ranges between 32 and 45 wt% while, inversely, CaO ranges between 16 and 26 wt%, corresponding to approximately 30–40 wt% of carbonate. As expected, the chemical composition clearly reflects the relative abundance of carbonates, either as clasts or in the matrix. Microprobe analysis indicates that the carbonate phases are all low in Mg-calcite with minor amounts of FeO (<0.1 wt%). The feathery carbonate fragments contain no detectable MnO, which agrees with its lack of luminescence (Heuschkel et al. 1998).

Middle Suevite (Clast-Rich Suevite)

This level is characterized by a higher concentration of larger clasts ranging in size between 2 and 5 mm enclosed in a fine-grained matrix (Figs. 2 and 3). Here, the clasts can be distinguished clearly from the more compact matrix. The size of the clasts and the proportion of basement material increases significantly compared to the upper suevite (Fig. 2). No specific fragment-poor or fragment-rich areas exist, with the exception of one part of the Y6 N14–6 sample, which is unusually rich in calcite (50%). The clasts are mostly composed of gneiss, quartzite, schist, carbonate, anhydrite, silicate melt particles, quartz and clay minerals (Fig. 3). The different clasts are not well-distributed throughout the rock, and locally, their relative proportions can vary significantly.

Most silicate basement fragments are altered to some degree, and the precise identification of their lithologies is often problematic. However, the most common lithologies seem to

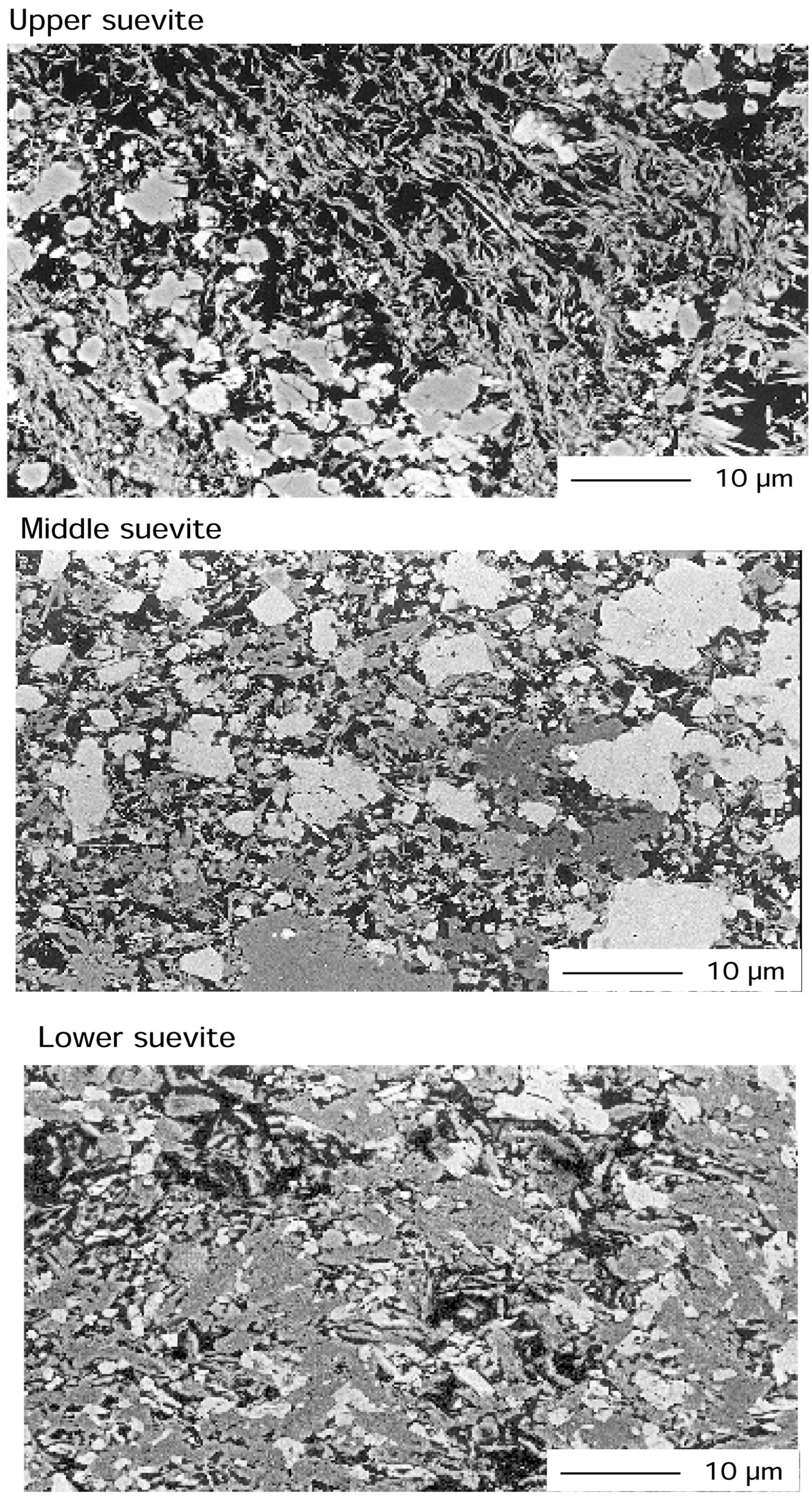

Fig. 4. Scanning electron photomicrograph, in backscattered electron mode, of the 3 types of suevite matrix. Notice the pore space filled with secondary clay minerals in the upper suevite and the calcite (light grey) and quartz (dark grey) grains. The matrix of the middle suevite with a high proportion of subrounded to rounded carbonate crystals (lighter color), quartz (dark grey), and feldspars (intermediate grey). Less porosity exists than in the overlying unit. The annealed and compact matrix of the lower suevite is clearly distinguishable with its amalgamated minerals (feldspar dark grey and pyroxene lighter grey). Locally (upper left), the primary clastic texture can still be recognized.

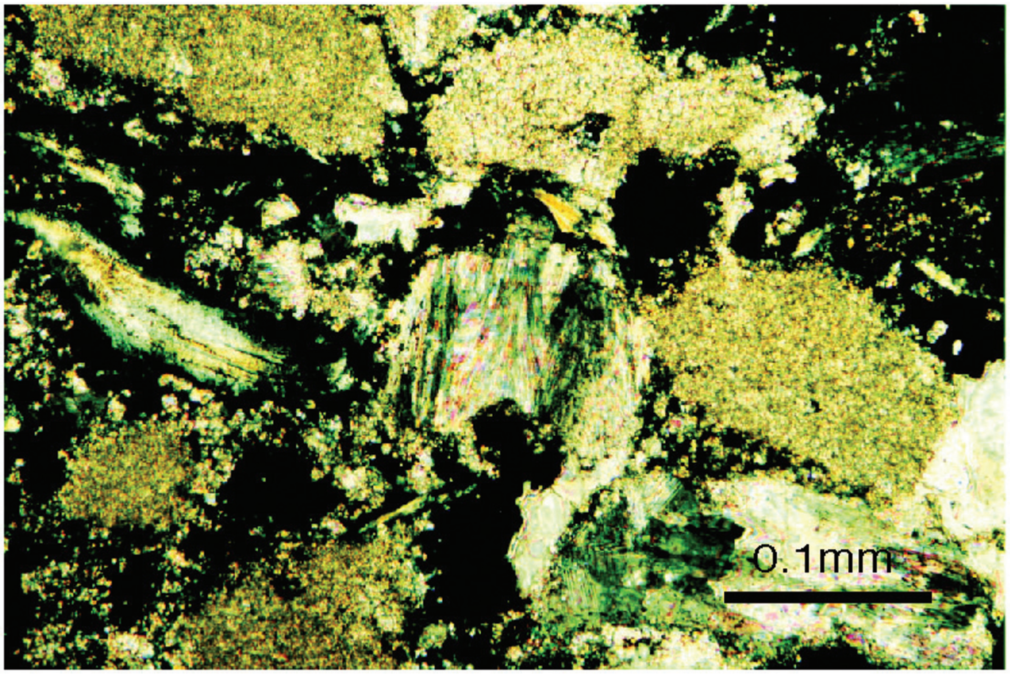

Fig. 5. Finer fraction of the calcite grains displaying the feathery texture indicative of rapid quenching from a melt in the upper suevite (crossed polars).

be gneissic and quartzitic. Greenish schists are less frequent and often clearly occur together in a restricted zone of the thin section, as if they orginated from the breaking of a larger clast. 45% of the clasts are relict crystalline basement clasts. Rare, dark brown fragments with a microcrystalline matrix and fluidal texture also occur; they might be clast of rhyolite, which occurs in the Yucatàn basement (Lopez-Ramos 1975). Alternatively, they could also represent another altered phase of the microcrystalline fragments of impact melt. A few quartz fragments display several sets of PDFs or mosaicism indicative of shock metamorphism. If evidence for shock effects increases at this level, it is still not widespread. Anhydrite often forms the largest clasts, but they represents only a few percent of the population. Some anhydrite clasts form separated aggregates of elongated prismatic crystals, which are, in many cases, associated with some opaque material composed of sulfides and/or organic matter. These unusual anhydrite aggregates differ from the typical crystalline forms of anhydrite identified below. Their $CaSO_4$ composition is confirmed by electron microprobe analysis. Cathodoluminescence study shows that the anhydrite aggregates do not display any luminescence.

Clasts of dark carbonate micrite, many of them with the same fossil assemblages described above, are present at this level. These carbonates represent less than 25% of the clasts. The feathery and sparry calcite crystals are rare, but some fragments of pure dolomite (±3% of the clast) occur in the middle suevite. This fine-grained dolomite resembles the blocks found in the diamictite breccia that marks the KT boundary in Belize, up to 360 km from the crater rim (Ocampo et al. 1996; Pope et al. 1999). They are probably derived from the Barton Creek dolomite member, or from an equivalent dolomite unit, which seems to have composed the upper part of the Yucatàn peninsula at the time of impact. At this distal site, this unit was eroded, reworked, and incorporated into the advancing ejecta blanket.

Subrounded green clay mineral fragments represent 20% of the clasts. They also probably represent altered melt fragments like the elongated clay mineral particles described above. Their degree of alteration is intense, they are often porous, and their chemistry seems more variable than the clay mineral particles in the overlying breccia (Table 1). They frequently contain minute carbonate (<5 μm) inclusions tightly embedded within the grain (Table 1). Better preserved microcrystalline melt fragments (Table 2) with a granodioritic-dacitic composition are also found. They can contain small recrystallized crystals of quartz. They average about <5% of the clasts, but they too can be found locally concentrated. These melt particles have higher FeO, CaO, and MgO and lower K_2O contents than their equivalent in the upper suevite (Table 1).

On average, the clastic matrix represents ~30% of the rock. It consists of angular to subangular small calcite grains (<10 μm) closely surrounded by a mixture of rounded K-feldspar, plagioclase, and quartz (Fig. 4). In some places, the carbonate and feldspar phases are in close contact, probably due to mechanical and diagenetic loading. Based on SEM point counting, the amount of calcite in the groundmass averages 40%, and bimodal grain size distribution is observed (10 μm and 1–3 μm). In comparison to the upper suevite, the quartz content is lower (5%), while K-feldspar (28%) and plagioclase (25%) contents are higher. Curiously, the amount of carbonate clasts decreases, but the proportion of $CaCO_3$ in the matrix has increased. The matrix is more abundant than in the upper suevite, and the porosity decreases to less than 10 vol%. The average size of the pore space is only a few microns, and secondary pore-filling phases such as zeolites and clay minerals are much less common than in the upper suevite. At this level, the form of the pores does not support a phase replacement process.

Bulk rock XRF analyses of the middle suevite indicate that major and trace element concentrations are less variable than in the overlying upper suevite (Table 3; Fig. 6). They also reflect the increase in basement components. The carbonate and anhydrite contents are estimated to be around 20 wt% and up to 2 wt%, respectively. These values agree with those obtained by the point counting method in thin sections. No anomalous concentration in platinum group elements was detected in this part of the suevite (Claeys et al. 1995).

Lower Suevite (Thermometamorphic or Annealed Suevite)

Below 1253 m, the Pemex well Y6 sampled the lower suevite with shocked basement clasts and abundant silicate melt particles (Figs. 2 and 3). Pristine basement clasts can still be recognized, but many display a high degree of alteration (Fig. 3). The majority of the clasts have a quartz or feldspar composition. Some gneiss and quartzite fragments can still be identified. Many fragments are partly or, often, completely digested in the matrix. A rim of clinopyroxene crystals, comparable those described by Kring and Boynton (1992) in the melt fragments of the underlying Y6 N17 unit, surrounds many of the quartz and feldspar clasts. The indication of shock metamorphism in both quartz and feldspar is clearly more common than in the other 2 types of suevite. Some quartz grains display clear indications of shock: sets of multiple PDFs and mosaicism. At least 15% of the clasts are shocked. A few clasts (>1 mm) of anhydrite are present at this level. The exact proportion of anhydrite is difficult to estimate as some of the observed fragments are obviously part of larger clasts that exceeded the diameter of the core. Nevertheless, this level contains more anhydrite than the other 2 suevites. Carbonate fragments were not observed; however, secondary carbonate veins do occur. The bulk composition clearly reflects the dominance of silicate basement components (Table 3).

Elongated melt clasts, up to 1 mm in size, occur (Fig. 3) locally with recrystallized quartz in their center. Alteration to

Table 3. X-ray fluorescence bulk rock analyses of the Chicxulub suevite. The analyses of the lower suevite was carried out in a zone devoided of the large anhydrite clasts.[a]

	Upper suevite			Middle suevite								Lower suevite
wt%	N13–3	N13–4	N13–9	N14–1	N14–5a	N14–5b	N14–10	N14–11a	N14–11b	N14–14	N14–15	N15–10
SiO_2	42.8	45.2	32.7	46.6	52.0	51.4	50.9	50.9	48.3	50.2	49.8	59.6
TiO_2	0.4	0.4	0.3	0.4	0.4	0.5	0.4	0.5	0.4	0.5	0.4	0.5
Al_2O_3	9.8	9.5	7.7	10.4	11.2	11.8	11.0	11.7	10.7	11.1	11.0	13.1
Fe_2O_3	4.1	4.0	2.9	4.5	4.3	4.3	4.4	4.7	4.4	4.4	3.9	5.3
MnO	0.1	0.1	0.1	0.1	0.1	0.1	0.1	0.1	0.1	0.1	0.1	0.1
MgO	5.4	4.9	4.3	4.2	4.0	4.0	3.9	4.2	4.2	4.0	3.5	4.2
CaO	16.2	17.0	25.7	15.0	12.0	10.9	12.5	11.5	13.5	13.1	13.5	7.7
Na_2O	2.4	2.5	2.1	3.1	3.4	3.7	3.3	3.5	3.0	3.6	3.6	5.1
K_2O	1.3	1.8	1.1	1.4	1.7	1.7	1.7	1.7	1.7	1.7	1.7	2.2
P_2O_5	0.1	0.1	0.1	0.1	0.1	0.1	0.1	0.1	0.1	0.1	0.1	0.1
SO_3	0.6	0.5	0.8	0.5	0.2	0.1	0.4	0.2	1.0	0.5	1.3	0.2
CO_2	12.2	11.5	18.7	10.2	7.4	10.0	7.8	7.6	8.7	7.9	8.4	0.3
LOI	4.2	3.5	3.4	3.2	3.1	1.4	3.4	3.4	3.4	3.3	2.7	1.7
Sum	99.5	101.0	99.8	99.7	99.4	99.4	99.3	99.4	99.6	100.5	100.0	99.5
ppm												
Ba	334	360	242	355	373	332	344	410	379	379	335	338
Co	<15	<15	<15	<15	<15	<15	18	17	17	<15	<15	19
Cr	47	42	31	42	57	56	58	60	52	48	52	58
Cu	64	100	98	556	<30	<30	<30	<30	65	181	81	<30
Nb	13	11	12	13	16	13	12	13	14	15	13	13
Ni	<15	<15	<15	<15	<15	16	39	22	<15	<15	<15	21
Rb	27	40	20	30	37	28	28	32	40	41	35	43
Sr	553	529	699	381	400	383	348	404	423	386	359	278
V	84	72	56	91	86	95	102	97	91	87	88	101
Y	<10	<10	<10	<10	10	12	<10	12	13	10	<10	16
Zn	46	<30	<30	49	43	40	51	47	53	39	<30	58
Zr	95	102	84	129	113	117	104	126	116	119	108	127
$CaCO_3$ (%)	27.7	26.0	42.0	23.2	17.0	23.0	17.7	17.3	20.0	18.0	19.0	0.7
$CaSO_4$ (%)	1.0	0.9	1.4	0.9	0.3	0.2	0.4	0.3	1.7	0.9	2.2	0.3

[a]Analytical conditions: 600 mg glass beads, LOI* = lost of ignition (LOI) after CO_2 determination; $CaCO_3$ and $CaSO_4$ are calculated.

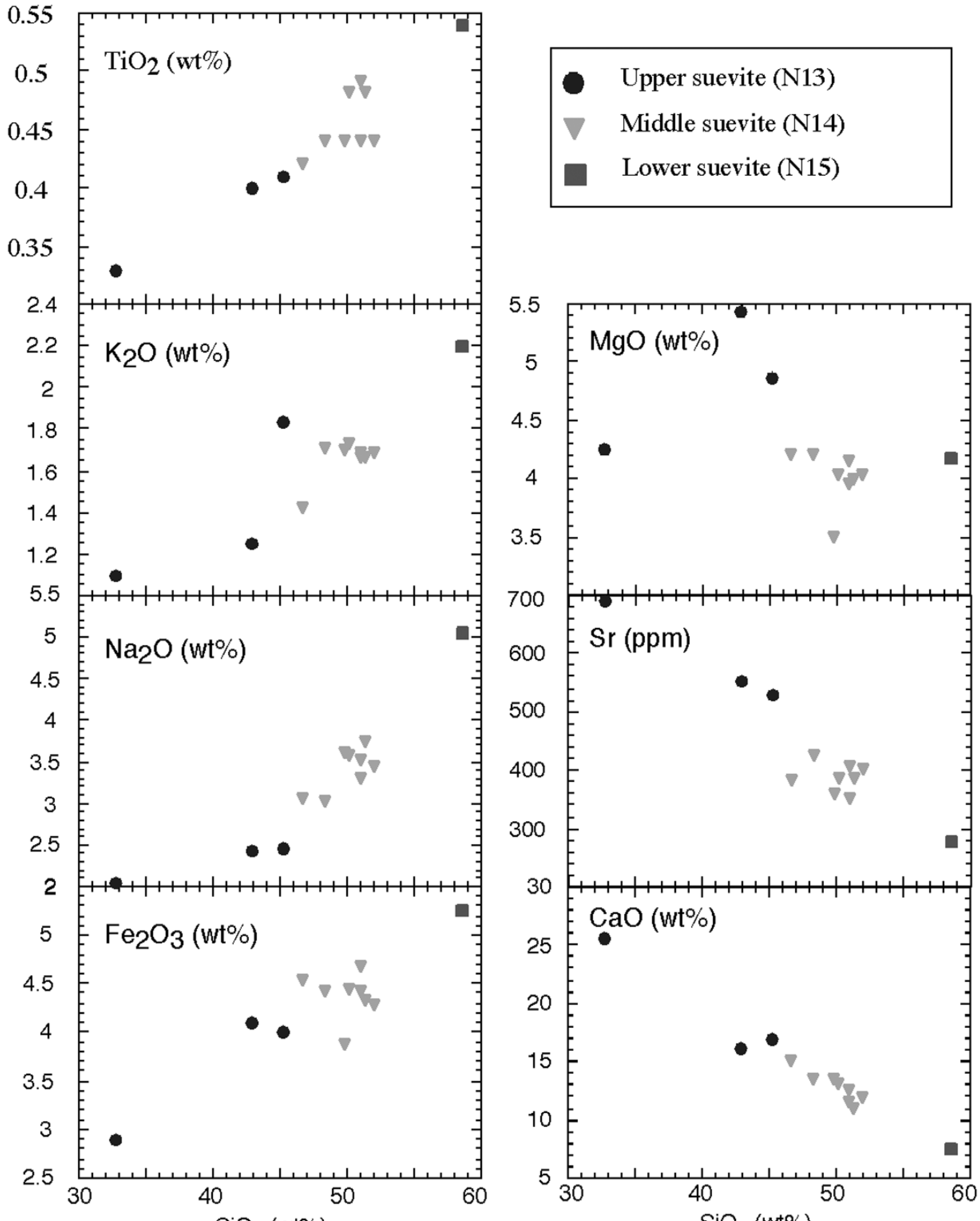

Fig. 6. Plots show the concentration of selected major, minor, and trace elements of the 3 parts of the Chicxulub suevite (bulk rock analyses, XRF). Notice the decrease in MgO, Sr, and CaO content and increase in TiO_2, K_2O, Na_2O, and Fe_2O_3 from upper to lower suevite with increasing depth.

clay mineral is less pronounced, the melt fragments are well preserved, and the fluidal texture is often visible. Dark and fine schlieren are detectable and appear to reflect chemical variations in SiO_2 and K_2O contents. The typical elongated clay mineral particles molded around clast are much less common. The melt clasts are isolated or occur as aggregates, as if they were stuck together. The amount of well-preserved silicate melt fragments is between 15 and 30% in some thin sections, the highest concentration of the whole suevite breccia sequence. Their average major element composition is given in Table 2.

At this level, the matrix is clearly not clastic anymore but is now formed of tightly packed intergrown minerals (Fig. 4), such as alkali feldspar (20%), plagioclase (56%), augitic pyroxene (18%), and quartz (5%). These proportions are based on point counting analyses but can vary significantly across a single thin section. Parts of the matrix appear to be fused togetherm while at other locations—often close to larger clasts—the formerly clastic features of the matrix can still be recognized. In some aspects, the groundmass appears much more similar to that observed in the underlying impact melt breccia just 40 m below in core fragment N16 (1293 m) than to the clastic matrix found in the overlying suevites. However, in the sample of impact melt breccia N17 and N19, the crystallized matrix seems almost perfectly to envelop and mold the clasts (Kring and Boynton 1992; Warren et al. 1996). In the lower suevite, one can still locally recognize that these contacts were more irregular with small voids, as expected for a formerly clastic matrix. The amount of calcite in the matrix is negligible (less than a few percent). No sorting is observed, and porosity drops to less than a few percent. The rare pores are, on average, around 2 microns in size and free of secondary pore filling phases (Fig. 4). Pyroxene crystals are nearly euhedral to subhedral and enclosed by anhedral alkali feldspar crystals.

DISCUSSION

Composition and Texture of the Suevite

The Chicxulub suevite is clearly different from the typical suevite reported at other, smaller impact structures. It is more heterogeneous in the overall texture, clasts and matrix composition, proportion of melt material, and shocked basement clasts. The chemistry and petrography of the samples from the three units (Y6 N13, N14, and N15) of well Y6 suevite breccia are variable and reflect the stratification of these units (Fig. 3). The contribution of the upper part of the target rock, both as clasts and in the matrix, decreases with depth. The amount of carbonate clasts and the bulk content of CaO, MgO, and Sr decrease with depth (Fig. 6). Silicate basement clasts and characteristic elements such as TiO_2, FeO, Na_2O, and K_2O increase in the lower parts of the suevite (Figs. 2 and 6). Anhydrite also appears more common in the lower suevite unit. Melt fragments and evidence of solid state shock metamorphism also increase with depth.

Texturally, the middle unit of suevite is most similar to suevite as defined and observed in other craters. The upper suevite unit is rather unique because of the fine grain size and its carbonate-rich character. The importance of carbonates in this unit, and, thus, perhaps also in the whole Chicxulub cratering process, is illustrated by the fact that carbonates are present as solid clasts, fine clastic matrix, and former melt phases. The lower suevite can be viewed as an intermediary unit between "classic" suevite of N14 and the underlying impact melt breccia already described by Kring and Boynton (1992), Schuryatz et al. (1994), and Warren et al. (1996). It appears to have reacted with the underlying hot melt-rock breccia, resulting in the annealing of its originally clastic matrix. The upper and the lower units seem to be lacking, or they have not been described characteristically in medium and small sized craters.

For various reasons, the fact that the Chicxulub suevites are distinctly different from those of the Ries crater is not surprising. Although the top sections of the targets of both craters are composed of carbonate rocks, the ratio of the thickness of the carbonate cover to the excavation depth is about 0.2 for Chicxulub and 0.06 for Ries. In addition, the Ries crater is an order of magnitude smaller (25 km in diameter) than Chicxulub. The suevite of the Nördlingen 1973 drill core located, as is the case for Y6 at Chicxulub, inside the transient cavity does not show any stratification of the type observed in Y6 (Stöffler et al. 1977). Carbonate clasts are completely lacking in the suevite of the Nördlingen drill core, and the total amount of clasts derived from the deep section of the sedimentary cover (Stöffler et al. 1977; Graup 1999) is very small (<0.2%). We must conclude that the central ejecta plume of Chicxulub is much more complex than that of Ries, where most of the relatively thin carbonate cover is removed by vaporization during the penetration of the projectile. Contrary to the Chicxulub case, in Ries, the ejecta plume is formed almost exclusively of vaporized, molten, and comminuted crystalline basement rocks, which are expelled vertically and redeposited more or less vertically, forming the fall-back suevite of the central depression. Outside the Ries crater rim, the thin and patchy suevite layer does contain a slightly higher fraction of sedimentary clasts, including carbonates (<1%). This is less than what is observed in the Chicxulub suevite. Another important difference between Chicxulub and Ries results from the fact that the volumes of vapor and melt do not scale linearly with increasing size of the crater (Grieve and Cintala 1992; Pierazzo et al. 1997). This will be discussed below.

The more than 200 km diameter Sudbury crater in Canada is the best candidate for an analogue of the Chicxulub suevites (Pye et al. 1984; Stöffler et al. 1994; Deutsch et al. 1995). The target of Sudbury comprised some 5 to 10 km of Proterozoic metasediments and volcanics (Huronian Supergroup) on top of Archean basement gneisses. The more than 1500 m thick suevite breccia unit, known as the Onaping Formation, is also clearly stratified regarding texture but not with respect to chemical composition. It is divided, from top to bottom, into aquatic "suevitic" sediments with carbonaceous matrix (Upper Black member), a reworked suevite breccia with carbonaceous matrix (Lower Black member), a melt-rich suevitic fall-back layer (Green member), a suevitic clastic matrix breccia (Gray member), and a clast-rich impact melt agglomerate with suevitic parts (Avermann 1994; Stöffler et al. 1994). The geologic setting of this sequence of clastic impact breccias and melt rocks is assumed to represent the central impact basin inside the (now eroded) peak ring of the Sudbury structure, in contrast to the Y6 well of Chicxulub, which is located outside of the peak ring. In spite of this, some similarities between both impactite units are obvious. The Sudbury Basal member is thermally annealed by the underlying coherent and hot impact melt sheet (Sudbury Igneous Complex) (Stöffler et al. 1994), an analogy to the lower suevite unit at the Y6 well of Chicxulub. Despite their different modes of formation, both units, perhaps, can be seen as intermediary or transitional between suevite and impact melt lithologies. The Grey member is texturally analogous to the middle suevite, and the Black member is, to some degree, comparable to the upper suevite unit of Chicxulub, which may also have been deposited in depositional environment as water rushed back within the cavity. No analogy to the Green member at the Y6 location exists, possibly also due to the incomplete sampling of Y6. In addition, some specific textural characteristics found in the Y6 impactite sequence are similar to observations made at the Onaping Formation such as corrosion of clasts and reactions rims around quartz and feldspar clasts, as well as alteration of melt particles to chlorite-rich clay minerals.

A comparison of the bulk chemistry of the suevites from Chicxulub, Ries, and Sudbury clearly reflects the important role of the 3 km thick sedimentary cover at Chicxulub compared to Sudbury and Ries, where carbonates are lacking or form a very thin cover, respectively. Only the lower Chicxulub suevite is compositionally similar to the suevites from Ries and Sudbury, reflecting the contribution of the deeper crystalline basement. In Chicxulub, the 3 types of suevite observed differ in grain size, bulk composition, clast proportion and origin, intensity of shock metamorphism, and in the type and mineralogy of the matrix. Chicxulub, because of its special target stratigraphy, is unique in showing that the sedimentary portion of the target rock strongly influences the composition of the fall-back suevite of a large impact structure. Shocked, melted, and pulverized limestone and probably dolomite, thus, formed a major component of the Chicxulub debris cloud and must have affected the chemical reactions taking place in this expanding plume. The amount of deeper basement components, such a gneiss, quartzite, and schist, but also apparently evaporite, increases significantly in the middle and especially in the lower suevite unit reflecting the primary stratigraphy. The basement lithologies identified correspond to those recognized by Lopez-Ramos (1975) in the various drillings carried out across the Yucatàn peninsula.

The suevite sequence is also stratified in terms of melt distribution and shock metamorphism. This reflects gradients in temperature and pressure conditions in the basement shortly before the excavation took place and different sources of material for the various units. Carbonate and silicate melts occur together in the upper suevite, which is depleted in solid basement clasts. In the middle suevite, solid clasts dominate over melt phases, and only silicate melt is again abundant in the lower unit. Abundant shocked features are found only in the lower suevite. However, this may be due, in part, to the fact that shock effects are much better constrained for quartz and feldspar (Stöffler and Langenhorst 1994) than they are for carbonates. We cannot be excluded that the clear sparry calcite found in the upper suevite represents shocked limestone grains, as has been speculated for similar grains identified in the KT ejecta unit in NE Mexico (Claeys et al. 1996). Preliminary microprobe analyses indicate that zones within these grains contain an excess of CaO (58 to 60 wt%) compared to stoichiometric carbonates. That this excess is widespread and possibly related to partial degassing of CO_2 remains to be demonstrated. Obviously, further work is required to characterize the shocked features in carbonates.

Carbonate Melts

So far, carbonates have often been neglected in studies of impactites. However, carbonates are common at the surface of the earth and, by consequence, in target rocks. Many more impactites must contain solid and melted carbonate phases (see Graup [1999] and Osinski and Spray [2001] for the Ries and Haughton craters, respectively). In the Chicxulub case, the contribution of carbonates to the produced melts was first attested by the presence of CaO-rich impact glass in the ejecta unit forming the base of the KT boundary clastic sequence in Mexico and Haiti (Izett 1991; Kring and Boynton 1991; Sigurdsson et al. 1991; Smit et al. 1992; Claeys et al. 1993; Bohor and Glass 1995; Claeys et al. 1998). KT boundary impact glasses range in composition from andesitic to CaO-rich (30 wt%). This compositional sequence is interpreted to be derived from the mixing of melted carbonate sediments with basement from the Yucatàn Peninsula (Bohor and Glass 1995). This implies that silicate and carbonate liquids were miscible under the temperature and pressure conditions prevailing in the environment where the ejecta plume formed. Experiments on liquid immiscibility (Lee and Wyllie 1996; Kjarsgaard 1998) show that, with increasing pressure, the immiscibility field broadens and the stability field of carbonate melt increases drastically, while the stability field of silicate melt gets very small at 2.5 GPa (Lee and Wyllie 1996). On the other hand, high pressure and temperature experiments on carbonate liquids by Moore and Wood (1998) show that, at 3 GPa and temperatures between 1475°C and 1525°C, the SiO_2 content dramatically increases, while the CO_2 content decreases, even up to temperatures >1700°C. All liquids then appear to be miscible. Immiscibility and miscibility of silicate and carbonate melts are key factors in the Chicxulub cratering event.

In the Ries suevite, Graup (1999) identified several signs of liquid immiscibility between silicate and carbonate melts, such as carbonate globules in silicate glass, menisci between carbonate and silicate melts, fluidal texture, and carbonate schlieren. Comparable features can be recognized in the Chicxulub suevite, where silicate and carbonate melts are often closely associated. The most common indication for carbonate-silicate immiscibility is the presence of elongated needles and spherules of carbonates in the silicate melt fragments. However, these can be difficult to identify due to the alteration of the melt to clay minerals. What is apparently even more common are solid carbonate fragments, some with possible fluidal textures or morphologies, completely engulfed by a thin layer of melt. The silicate melt is wrapped around the carbonates as would be expected if the 2 phases came in contact and quickly cooled while closely sticking together. No equivalent to the ejected CaO-rich impact glass observed at proximal KT-boundary sites was found preserved in the fall-back suevite. Thus, no indication exists that the silicate and calcite melts were fully miscible in the formation environment of the suevite. This could be due to the fact that, in the central part of the crater where a vertical flow field dominates, carbonate melt and underlying silicate melt were not mixed. The upper suevite has formed and then cooled under pressure/temperature conditions that favored the immiscibility of silicate and carbonate melts.

The feathery calcite, which is diagnostic for rapidly quenched carbonate liquid, is present essentially in the upper part of the Chicxulub suevite (Fig. 5). Feathery calcite is known from carbonatite lavas (Keller 1981, 1989) and from laboratory experiments, where it forms under quenching rates of ±400 degrees per second (Hamilton et al. 1979; Jones and Wyllie 1983; Wyllie 1989; Jones et al. 1998). Even at extreme rates, carbonate melts do not quench to glass (Genge et al. 1995). The feathery calcite grains and their formation processes in the Chicxulub Y6 suevite are described in detail by Jones et al. (2000). The abundance of feathery calcites indicates that a significant volume of carbonate melt was produced by the Chicxulub impact. In the upper part of the suevite, the feathery-melt phase accounts for at least 15% of all the carbonate clasts, that is, counting the large and small crystals described above. This value is higher than that the 10% initially proposed by Jones et al. (1999), who had based their estimation only on the larger feathery calcite crystals. This calcite melt phase is more or less absent in the other 2 suevite members. Using a conservative extrapolation, Jones et al. (2000) estimated that the total carbonate melt volume produced in Chicxulub was between 100 and 300 km^3. In view of the present study, the higher estimation of 300 km^3 must now be favored. This value still excludes the carbonate melt that was incorporated in the yellow impact glass found at the KT boundary all over the Gulf of Mexico region.

Molten silicate and carbonate phases are essential components of both the suevite upper members and the impact glass ejected outside the crater. These molten materials presumably originated at different depths and locations within the evolving crater. They were then brought together in the turbulent debris cloud as it rose above the crater. However, a clear segregation remained between the parts of the cloud where there was ejecta glass and where there was material that fell back vertically as the upper suevite formed. The first zone was probably hotter so that the 2 liquids became miscible. The suevite formed in a zone prone to rapid quenching of the liquid carbonates, as demonstrated by the presence of feathery calcite and possible silicate-carbonate immiscibility. These conditions, perhaps, were fulfilled as the molten material fell back or was expelled from the more central part of the cloud. These processes could also happen as the 2 liquids entered a zone, possibly more external, dominated by the colder carbonate fragments, such as the micritic grains with fossils. Such fragments are abundant in the upper suevite and clearly never experienced high temperature conditions. This would also explain the carbonates "sheathed" by silicate melt. Rapid quenching also may have happened as the particles fell back into the crater, perhaps as it began to fill with back-washing seawater.

Evaporites in the Target Rock

The evaporites are supposed to have released large volumes of sulfur components (SO_X) to the atmosphere upon shock vaporization (Pope et al. 1994; Ivanov et al. 1996; Pierazzo et al. 1998; Yang and Ahrens 1998; Gupta et al. 2001). However, the precise degassing conditions of evaporites are even more complex and less known than those of carbonates. Sulfur-volatile outgassing begins at the release from 30 to 40 GPa shock loading and is completed at 60 to 80 GPa (Badjukov et al. 1995). Recovery experiments by Ivanov et al. (1996) show no decomposition of anhydrite shocked at 63 GPa. Reliable values of shock pressures required for partial or complete anhydrite decomposition are still not available. Similar to shock experiments on carbonate material (Martinez et al. 1995), the newly formed CaO may have reacted with available SO_3. If this reaction took place in the ejecta plume, it may decrease the amount of outgassed sulfur material significantly (Ivanov et al. 1996; Martinez et al. 1994; Martinez et al. 1995).

Lopez-Ramos (1975) estimated that evaporites represented between 23 and 60% of the Yucatàn sedimentary sequence in the Late Cretaceous. These values are more often based on geophysical logs acquired during or after the drilling and on well cuttings rather than on direct sample observations. Based on the Lopez-Ramos values, Ivanov et al. (1996) calculated a total amount of 3×10^{16} g to 3.8×10^{17} g of sulfur delivered to the atmosphere. However, if the clast proportion in the suevite reflects the proportion of target lithologies, then the evaporite fragments are much less common in the suevite recovered in well Y6 than expected based on Lopez-Ramos (1975) data. In the upper and middle suevite, the ratio between carbonate and evaporite clasts is typically less than 5:1. No evaporite occurs in the matrix at any level, unless, as speculated above, the larger pores observed in the upper suevite represent a now dissolved gypsum of anhydrite component. Even if this was effectively the case, the amount of evaporite in the upper suevite unit would not significantly increase. The less than 5:1 carbonate-evaporite proportion agrees with the stable isotope analyses of Blum and Chamberlain (1992) on the ejected impact glass. Their data show that the different glass compositions fall on a mixing line between an isotopically heavy Ca-rich composition and a lighter silica composition, allowing only a ±10% contribution of evaporitic material. Koeberl (1993) came to a similar conclusion based on trace element analysis of the impact glass. Alone, this set of data may be taken as an indication that the evaporite proportion affected by the impact event is much less than previously considered (Claeys 2000).

However, the carbonate versus evaporite ratio is not uninform over the whole suevite sequence. In the lower suevite member, the proportion of evaporite clasts seems to increase and could reach 15 or even 20% of the clasts. However, these values could be biased by the presence of a few isolated large evaporite clasts, the sizes of which exceed the diameter of the Y6 core. Thus, whether this increase is due to the presence of a real-evaporite unit within the suevite or just the result of a few randomly distributed large evaporite blocks is difficult to determine. Based on point counting analysis, the underlying melt rock (sample Y6 N17 and 19) contains anhydrite clasts but in a proportion that does not exceed 15% of the clasts. Based on the limited samples available from well Y6, the vertical extension of this evaporite-rich layer is not possible to determine. The estimation of the proportion of anhydrite is further complicated by the fact that Y6 bottoms in anhydrite (Lopez-Ramos 1975). This anhydrite could be a large block encompassed in the melt rock. Although unlikely considering the position of Y6, we cannot rule out that these layers are part of the Yucatàn pre-impact stratigraphy.

At this depth, carbonates are absent as clasts and in the matrix. Again, this reflects the initial stratigraphy of the Yucatàn target rock. Lopez-Ramos (1975) placed the thicker evaporite layers at the bottom of the 2 to 3 km of sedimentary cover. However, the UNAM 6 and 7 wells drilled just outside the crater rim, some 90 km away, encountered stratified evaporite at less than 700 m depth (Urrutia et al. 1996). More data is required from other locations in the crater to access the precise extend of the evaporite. Another explanation for the low proportion of evaporite clasts in the upper suevite units may be that, at this level, the evaporite layers were completely shock-vaporized by the impact. The unusual anhydrite aggregates found in the middle and lower suevite, thus, would perhaps represent recrystallized anhydrite melt, similar to the feathery calcite described in the upper suevite.

Based on these contradictory lines of evidence, i.e., the uncertainty concerning the distribution and stratigraphy of the evaporite units in the target rock, and the uncompleted knowledge of the conditions required for shock decomposition of evaporites, the volume of SO_X components released by the impact remains difficult to constrain precisely. Sulfur components are now considered to be the major (and, perhaps to some extreme, only) factor driving the climatic perturbation (e.g., Pope 2002). The information extracted from the Y6 core shows that using the conservative estimation of 15% (to maximum 20%) evaporite in the target rock is safe when modeling the effects of the KT boundary impact. If the lack of evaporite in the upper suevite units reflects the almost complete vaporization of the evaporite layers, the proportion of S-rich components released by the Chicxulub impact event could easily double.

Silicate Melt

Two chemically different silicate melts occur in the upper part of the suevite (Table 2). In the upper suevite, the melt has a feldspathic composition. The FeO, MgO concentrations are low, and the amounts of K_2O and Na_2O are highly variable, as is typical for altered glasses. In general, silicate melt fragments in the middle suevite and in the lower suevite are chemically more mafic (i.e., they contain higher amounts of FeO, MgO, and CaO). The 2 melts might be derived from different initial basement target rock compositions. If the stratigraphy of the Chicxulub suevite reflects the lithological sequence of the target rock, on can assume that the upper part of the Yucatàn basement is dominated by more feldspar-rich rocks like granites and/or felsic volcanics. This assumption is corroborated by the stratigraphic reconstructions of Lopez-Ramos (1975) and the finding of rhyolite fragments in the middle suevite. At the thin section scale, the melt fragments show more compositional variability than those from most other impact structures. Along with the compositional differences, some of the melt is relatively fresh and pristine, while other phases are completely altered to clay minerals. The fact that several kinds of melt can coexist in one sample leads to the conclusion that no widespread homogenization of the melt occurred.

Most other medium to large impact craters on Earth do not display such a heterogeneous melt composition and especially not with such small scale variations (<2 cm). This is probably due to either their smaller sizes and/or the fact that, at all larger craters (>25 km in diameter) formed in crystalline rocks or in mixed targets with crystalline basements, the surficial impact formations inside and outside the crater are completely eroded. The observed melt heterogeneities possibly reflect: 1) a complex process of vaporization, melting, mixing of liquid and solid components, and ejection; 2) a lack of homogenization of the ejecta melts; and 3) an even more complex target lithology than proposed by Lopez-Ramos (1975) and deduced from the clasts composition. The lower part of the target rock must have consisted of more mafic lithologies. Kring and Boynton (1992) had reached a similar conclusion based on a petrological study of the underlying melt rock found in Y6. Kettrup et al. (2000) advocated the presence of an intermediate to mafic precursor based on their Rb-Sr and Sm-Nd analyses of the impactites from the Y6 and Chicxulub 1 wells. Despite a detailed search, no (convincing) mafic clast was found. Considering the scale of the Chicxulub crater and the somewhat limited knowledge of the composition of the Yucatàn Pan-African basement, the observed heterogeneity is not at all surprising. The Chicxulub impactites offer a window on the composition of the deeply buried Yucatàn basement.

Differences in the Groundmass

Major differences are found in the composition of the fine groundmass in the 3 different Chicxulub suevites (Fig. 4). In the upper and middle suevite, the groundmass is a clastic matrix, characteristic of suevite as defined in the Ries crater, for example. In the upper suevite, the occurrence of gedrite, an orthoamphibole, in the groundmass can be explained by the possible reaction involving chlorite and quartz and/or plagioclase under metasomatic conditions after the impact (Deer et al. 1993). The hydrothermal circulation responsible for the generation of such secondary phases is likely fueled by the underlying slow-cooling impact melt rock (Kring and Boynton 1992). The modeling of such a hydrothermal system indicates that it could remain active for up to 10^5 or 10^6 years (Abramov and Kring 2003). It is also the cause of the secondary anhydrite and carbonate replacement observed in veins and fractures. This circulation may be responsible for the dissolution of the unidentified matrix component, which left the larger well-defined pore spaces in the upper suevite and the partial filling with secondary cobweb-morphology clay minerals and zeolites. The middle suevite is clearly more compacted, perhaps by the loading effect of the above lying unit. The higher calcite content and the bimodal size distribution of the calcite in the matrix of the middle suevite may support two processes of formation: as clastic matrix for the larger fraction, and for the finer grains, as a diagenetic precipitation after emplacement of the suevite. Here, the form of the pores does not support a phase dissolution process. Pore spaces (<20 %) are less common, smaller, and not usually filled by a secondary phase replacement. The groundmass in the lower suevite differs significantly from the matrix in the upper and middle suevite and cannot be described as clastic (Fig. 4). It is completely recrystallized, most likely at the contact of the underlying hot impact melt. The first samples of impact-melt breccia are found some 40 m below in core fragment N16 (1293 m). Their matrix is similar to that observed in the lower suevite unit.

Emplacement of the Suevite

The proposed emplacement scenario must be viewed as a preliminary interpretation that is based on a limited set of samples taken from a more than 200 m thick unit of suevitic breccias. For the derivation of an emplacement model for these breccias, sources of information besides the petrographic and compositional data reported in the previous sections need to be taken into account: 1) the structural and geophysical setting of the Y6 drill core (Morgan et al. 1997); 2) the comparison with suevites from other terrestrial craters (e.g., Engelhardt and Graup 1984; Avermann 1994; Stöffler et al. 1994; Engelhardt 1997; Graup 1999); and 3) the results of numerical simulations of the Chicxulub impact (Alvarez et al. 1995; Pierazzo et al. 1998; Pierazzo and Melosh 1999).

First, Y6 is located in the inner part of the ring depression which surrounds the peak ring structure of Chicxulub. At this position, the following components can be expected: a) suevite-type material formed by ground surging on the wall region of the growing transient cavity, leading to a downward-inward material flow after transient cavity collapse and melt pool formation; b) fall-back suevite from the ejecta plume; and c) possibly, redeposited suevite formed by the inward moving ocean water after crater formation. Second, comparison with suevite formations at other terrestrial craters that are all smaller than Chicxulub, except for Sudbury (where the ring trough is completed eroded), clearly shows that the triple-layered suevite formation of Chicxulub is structurally and compositionally unique, indicating different and perhaps independent formation and emplacement processes. Third, the boundary conditions obtained by the numerical simulations of the Chicxulub impact are most relevant. In contrast to small craters such as the Ries, the ejecta plume of Chicxulub is extremely large (penetrating far beyond the stratosphere) and, hence, less turbulent (Kring et al. 1996). The different target materials (water, sedimentary layer, crystalline basement rocks) and the projectile contained in the ejecta plume appear to leave the crater sequentially, with the deepest material being the latest entering the plume (Pierazzo et al. 1998). These materials, mostly in the form of vapor and melt, to some degree, stay in separate zones of the plume for more than 30 sec (30 sec = maximum computation time). Moreover, the ejecta plume has a much larger lateral extension at low altitudes deviating distinctly in this respect from the mushroom type plume typical of smaller craters (Kring et al. 1996). In view of the above described information and boundary conditions, the 3 layers of suevitic breccias can be interpreted as follows.

The upper suevite is composed essentially of the carbonate rocks from the uppermost part of the target sequence. Vaporization, melting, and minor solid comminution products of the carbonate- and sulfate-rich sedimentary rocks started to raise immediately after the initial impact as part of the ejecta plume (see plates 1 & 2 in Pierazzo et al. [1998] and Pierazzo and Melosh [1999] for the temperature of the ejecta). Most of the unvaporized material remained on the outside of the ejecta plume as it rose. Because of turbulence in the outer parts of the plume, the unvaporized material may have interacted with some melted silicate material coming from the deeper central zone and spewed from the crater some 10–15 sec after the impact (Pierazzo et al. 1998). Apparently, few shocked and unmelted basement clasts originating at greater depth could reach the formation environment of the upper suevite, except as a micro-sized fraction incorporated in the matrix. The zone was hot enough for the carbonate and silicate melts to co-exist and to interact but not to the point where the 2 liquids became fully miscible. Considering an alternative model, this may also correspond to the zone where the CO_2-rich warm fireball described by Alvarez et al. (1995; Figs. 3c and 3d), in which carbonate clearly dominates basement clasts, interacted with the raising silicate-dominated hot fireball. In an case, the upper suevite material must have risen significantly, but never penetrated the hotter part of the raising plume before it settled back in the crater. If water was able to quickly backwash into the crater, it may have had to settle through the water column, as perhaps indicated by the faint lamination or layering texture surmised on some of the samples and by the overall small grain size compared to the much coarser middle and lower suevite layers. An alternative explanation is to view this fine-grained suevite as a late phase clastic aqueous deposit that was washed back into the outer ring trough from the crater rim deposits of Chicxulub when the ocean rushed back in immediately after the collapse of the transient cavity. The high abundance of silicate minerals in the matrix may be derived from the top layer of the late ejecta deposited at the crater rim region, which, according to the principle of inverted stratigraphy, was rich in basement material. This material originally may have been a kind fallout of suevite.

The formation of the middle suevite is more difficult to derive from the model calculations of Pierazzo et al. (1998), which are limited to 30 sec after impact. At this time, the transient cavity is near to completion (Roddy et al. 1987), but the ejection process and the expansion of the plume is not finished yet. For reasons discussed below, the middle suevite is most likely related to a later stage of the development of the ejecta plume. In contrast to the upper and lower suevite, the texture and composition of this suevite section is most similar to the typical fall-back suevite described in other, mostly smaller craters. This suevite obviously formed in a region of the lofted debris cloud that was dominated by basement rock material (melt and clasts of variable degree of shock) and that was highly diluted in the uppermost sedimentary target material, i.e., the sedimentary rocks, except for the finest fraction containing around 30% of pulverized carbonates (Fig. 4). The clast distribution seems to indicate that this suevite unit was not fully homogenized. The turbulence was, perhaps, too weak in this zone to completely mix clasts originating from different locations within the crater, either deep in the basement or outward from the growing transient cavity. Some silicate melt material still exists but almost no carbonate melt. Interactions between silicate liquids and carbonate clasts are also less pronounced, as if they came in contact when the silicates were already solid. The model of Pierazzo et al. (1998) seems to show that solid (unshocked and unmelted) basement rocks are thrown out at the periphery of the transient cavity before the flap of overturned target rocks is formed (Roddy et al. 1987, Fig. 4). In this zone, basement rocks are likely to interact with pulverized but solid carbonates lofted from the deepest layers of the sedimentary cover at the periphery of the forming crater. In any case, the material of the middle suevite, most plausibly, was deposited out of the ejecta plume as fall-back material. On the Alvarez et al. (1995) model (Fig. 2d), the unit may have formed slightly above the crater, where the trail of the expanding "warm" plume interacted with the ejecta curtain and deep solid basement material.

The lower suevite unit has undergone a rather different mode of formation. This unit is depleted in uppermost target lithologies and probably was never lofted very high above the growing crater floor, if it ever left the ground at all. In well Y6 (sample N16 at 1293 m), coherent impact melt breccia was encountered some 40 m below the lower suevite. At this point, the size and extension of the Chicxulub impact melt pool, in particular, are difficult to estimate, and answerering the question of how far it extended radially in the ring trough is also difficult (Sharpton et al. 1996; Pilkington et al. 2000). What is evident is that the lower suevite unit formed in close association with the underlying impact melt breccia and has been thermally metamorphosed by the hot sublayer. This must be concluded from the texture and mineralogical composition of the suevite matrix as described above (Fig. 4). The exact mode of emplacement of the suevite components is not yet fully understood. Either the material is early fall-back material from the lowermost part of the ejecta plume or it has been deposited by lateral inward movement of the ground-surged material of the outer cavity floor during collapse of the transient cavity. One could also speculate that the shocked and solid clasts were deposited on top of local melt ponds that had just started to form a thin crust at their surface. The lower suevite, thus, is viewed as a transition or contact unit between real suevite and the underlying impact melt breccia. The exact thickness of this unit cannot be estimated based on the available samples.

CONCLUSIONS

The detailed analyses and investigations of the Chicxulub suevite from the Y6 drill core show that the suevite is complex and heterogeneous in composition. Three different layered subunits of the suevite breccia could be identified. The proportion of carbonate and matrix porosity decrease with depth, while basement clasts and silicate melt increase. Indications of shock metamorphism are also more common in the lower suevite than in the units above. The upper part, which is rich in carbonate both as clasts and in matrix, is highly unusual. Two interpretations can be proposed: 1) the upper suevite layer represents a late fall-back material from the side of the uppermost part of the ejecta plume, which may have settled through the water column after the cavity was inundated shortly after crater formation; 2) the upper suevite layer is reworked marine sedimentary deposit transported to its present location immediately after crater formation by the highly dynamic erosion of the rim region by the ocean water rushing back into the crater. The middle suevite is considered to be a typical fall-back suevite that formed out of the central region of the collapsing ejecta plume. The lower suevite has been deposited either as early fall-back material from the lower central part of the ejecta plume or it was derived from source material deposited on the outermost flanks of the transient crater floor and was moved inward during the cavity collapse. After deposition, the lower suevite was affected by post impact thermal metamorphism induced by the underlying coherent impact melt breccia. The complete sequence of suevitic material in Y6 displays some alteration by post-impact hydrothermal processes.

The results of this study not only shed some light on the type and sequence of processes involved in the formation of the allochthonous impactite section in the ring trough of the Chicxulub crater but also open a window into the lithological sequence of the Cretaceous and the deep Yucatàn crystalline basement. Both types of information have significant implications for understanding how the released volatiles and dust perturbed the global Earth system and ultimately drove the mass extinction of organisms. The counting of evaporite clasts (anhydrite) and the examination of the matrix sets a lower limit of ~20% evaporite in the Yucatàn sedimentary cover, which is less than that used in several climate models (Pope et al. 1994; Ivanov et al. 1996; Pierazzo et al. 1998) to quantify the amount and type of volatiles injected into the atmosphere by the Chicxulub impact. Moreover, the presence of calcite melt in the suevite indicates that a significant portion (perhaps 15% or more) of the carbonate present in the upper part of the target was shock melted and not completed vaporized upon impact. This needs to be accounted for when estimating the quantities of CO_2 produced in the Chicxulub event as done by Pierazzo et al. (1998). One must also considere that anhydrite may have undergone a similar melting rather than a vaporization process. Melts of different compositions reflect the heterogeneity of the Yucatàn basement and demonstrate that no widespread homogenization of the melt took place.

These conclusions remain preliminary since they are based on a non-continuous sequence of small samples from a single well on the outer flank of the central peak ring (50 km SW). The results presented here may only be valid for the innermost part of the ring trough area. In the outer trough zone or toward the crater rim, the impactite composition could be different. The study of the suevite samples recovered by the International Continental Drilling Program (ICDP) at a more distal site will complement the present data, hopefully leading to a more complete characterization of the unusual Chicxulub suevite.

Acknowledgments–Part of this work was financed by an OZR grant from the Vrije Universiteit Brussel to P. Claeys. This research was initially supported by the Deutsche Forschungsgemeinschaft (DFG grants Cl 147/2–1 + Cl 147/2–2) in the framework of the DFG Schwerpunktprogramm ICDP/KTB to Philippe Claeys. Sabine Heuschkel was a postdoctoral researcher supported by this same DFG program (Grants Cl 147/2–1 and Cl 147/2–2). We thank Dr. Ralf Thomas Schmitt, Museum für Naturkunde, Berlin, for performing XRF analyses on Y6 samples. We also thank the Instituto Mexicano del Petroleo for providing sample material. Juan T. Vasquez-Ramírez kindly assisted with the sample preparations and A. M. Reyes Salas with the electron microprobe analyses at UNAM.

Editorial Handling—Dr. Richard Grieve

REFERENCES

Abramov O. And Kring D. A. 2003. Finite-difference modeling of impact-induced hydrothermal systems (abstract #1846). 34th Lunar and Planetary Science Conference. CD-ROM.

Alvarez W., Claeys P., and Kieffer S. W. 1995. Emplacement of KT boundary shocked quartz from Chicxulub crater. *Science* 269: 930–935.

Avermann M. 1994. Origin of the polymict, allochthonous breccias of the Onaping formation, Sudbury structure, Ontario, Canada. In *Large meteorite impacts and plantary evolution,* edited by Dressler B. O., Grieve R. A. F., and Sharpton V. L. Boulder: Geological Society of America. Special Paper 293. pp. 265–274.

Badjukov D. D., Dikov Y. P., Petrova T. L., and Pershin S. V. 1995. Shock behaviour of calcite, anhydrite, and gypsum (abstract). 26th Lunar and Planetary Science Conference. pp. 63–64.

Blum J. D. and Chamberlain C. P. 1992. Oxygen isotope constraints on the origin of impact glasses from the Cretaceous-Tertiary boundary. *Science* 257:1104–1107.

Bohor B. F. and Glass B. P. 1995. Origin and diagenesis of K/T impact spherules from Haiti to Wyoming and beyond. *Meteoritics & Planetary Science* 30:182–198.

Carroll M. R. and Webster J. D. 1994. Solubilities of sulfur, noble gases, nitrogen, chlorine, and fluorine in magmas. In *Volatiles in magmas,* edited by Carroll M. R., and Holloway J. R. Washington D.C.: Mineralogical Society of America. *Reviews in Mineralogy* 30:231–279.

Claeys P. 2000. What is exactly the role of evaporites in the Chicxulub event (abstract). In *Catastrophic events and mass extinctions: Impacts and beyond.* Houston: Lunar and Planetary Institute. Contribution No. 1053. pp. 24–25.

Claeys P., Alvarez W., Smit J., Hildebrand A. R., and Montanari A. 1993. KT boundary impact glasses from the Gulf of Mexico region (abstract). 24th Lunar and Planetary Science Conference. pp. 297–298.

Claeys P., Asaro F., Rocchia R. E. R. Hildebrand A. R., Grajales J. M., and Cedillo E. 1995. Ir abundances in the Chicxulub melt-rock (abstract). 4th International Workshop of the ESF Scientific Network on Impact Cratering and Evolution of Planet Earth. pp. 55–57.

Claeys P., Alvarez W., Smit J., and Montanari A. 1996. Shocked (?) limestone fragments—A new component of the proximal impact ejecta of the Chicxulub crater (abstract). *Meteoritics & Planetary Science* 31:A29.

Claeys P., Smit J., Montanari A., and Alvarez W. 1998. L'impact de Chicxulub et la limite Crétace-Tertiaire dans la région du Golf du Mexique. *Bulletin Société Géologique de France* 169:3–9.

Deer W. A., Howie R. A., and Zussman J. 1993. *An introduction to the rock-forming minerals.* 2nd edition. London: Longman Scientific & Technical. 696 p.

Deutsch A., Grieve R. A. F., Avermann M., Bischoff L., Brockmeyer P., Buhl D., Lakomy R., Muller-Mohr V., Ostermann M., and Stöffler D. 1995. The Sudbury structure (Ontario, Canada): Aa tectonically deformed multi-ring impact basin. *Geologische Rundschau* 84:697–709.

Engelhardt W. V. 1997. Suevite breccia of the Ries impact crater, Germany: Petrography, chemistry, and shock metamorphism of crystalline rock clasts. *Meteoritics & Planetary Science* 32:545–554.

Engelhardt W. V. and Graup G. 1984. Suevite of the Ries crater, Germany. *Geologische Rundschau* 73:447–481.

Flügel H. W. 1982. *Microfacies analysis of limestones.* Berlin: Springer-Verlag. 633 p.

Genge M. J., Jones A. P., and Price G. D. 1995. An infrared and Raman study of carbonate glasses: Implications for the structure of carbonatite magmas. *Geochimica et Cosmochimica Acta* 59: 927–937.

Graup G. 1999. Carbonate-silicate liquid immiscibility upon impact melting: Ries crater, Germany. *Meteoritics & Planetary Science* 34:425–438.

Grieve R. A. F. and Cintala M. J. 1992. An analysis of differential impact-melt crater-scaling and implications for the terrestrial impact record. *Meteoritics* 27:526–538.

Grieve R. A. F., Dence M. R., and Robertson P. B. 1977. Cratering processes: As interpreted from the occurance of impact melts. In *Impact and explosion cratering,* edited by Roddy D. J., Pepin R. O., and Merril R. B. New York: Pergamon Press. pp. 791–814.

Gupta S. C., Ahrens T. J., and Yang W. B. 2001. Shock-induced vaporization of anhydrite and global cooling from the K/T impact. *Earth and Planetary Science Letters* 188:399–412.

Hamilton D. L., Freestone I. C., Dawson J. B., and Donaldson C. H. 1979. Origin of carbonatites by liquid immiscibility. *Nature* 279: 52–54.

Heuschkel S., Lounejeva Baturina E., Jones A. P., Sanchez-Rubio G., Claeys P., and Stöffler D. 1998. Carbonate melt in the suevite breccia of the Chicxulub crater (abstract). *Eos Transactions* 79: F554.

Hildebrand A. R., Penfield G. T., Kring D. A., Pilkington M., Camargo Z. A., Jacobsen S. B., and Boynton W. V. 1991. Chicxulub crater: A possible Cretaceous/Tertiary boundary impact crater on the Yucatàn Peninsula, Mexico. *Geology* 19: 867–871.

Ivanov B. A. and Deutsch A. 2002. The phase diagram of $CaCO_3$ in relation to shock compression and decomposition. *Physics of the Earth and Planetary Interiors* 129:131–143.

Ivanov B. A., Badukov D. D., Yakovlev O. I., Gerasimov M. V., Dikov Y. P., Pope K. O., and Ocampo A. C. 1996. Degassing of sedimentary rocks due to the Chicxulub impact: Hydrocode and physical simulations. In *The Cretaceous-Tertiary event and other catastrophes in Earth history,* edited by Ryder G., Fastovsky G. D., and Gartner S. Boulder: Geological Society of America. Special Paper 307. pp. 125–140.

Izett G. A. 1991. K-T boundary tektites from near Beloc, Haiti (abstract). 24th Lunar Planetary Science Conference. pp. 625.

Jones A. P. and Wyllie P. J. 1983. Low-temperature glass quenched from a synthetic, rare earth carbonatite: Implications for the origin of the Mountain Pass deposits, California. *Economic Geology* 78:1721–1723.

Jones A. P., Heuschkel S., and Claeys P. 1998. Comparison between carbonate texture in Chicxulub impact rocks and synthetic experiments (abstract). *Meteoritics & Planetary Science* 33:A79.

Jones A. P., Claeys P., and Heuschkel S. 2000. Impact melting: A review of experimental constraints for carbonate targets and applications to the Chicxulub crater. In *Impact and early Earth,* edited by Gilmour I. and Koeberl C. Berlin: Springer-Verlag. *Lecture Notes in Earth Sciences* 91:343–362.

Katz K. and Keller J. 1981. Comb-layering in carbonatite dykes. *Nature* 294:350–352.

Keller J. 1981. Carbonatitic volcanism in the Kaiserstuhl alkaline complex: Evidence for highly fluid carbonatite melts at the earth's surface. *Journal of Volcanology and Geothermal Research* 9:423–431.

Keller J. 1989. Extrusive carbonatites and their significance. In *Carbonatites: Genesis and evolution,* edited by Bell K. London: Unwin Hyman. pp. 70–88.

Kettrup B., Deutsch A., Ostermann M., and Agrinier P. 2001. Chicxulub impactites: Geochemical clues to the precursor rocks. *Meteoritics & Planetary Science* 35:1229–1238.

Kjarsgaard B. A. 1998. Phase relations of a carbonated high CaO nephelinite at 0.2 and 0.5 GPa. *Journal of Petrology* 39:2061–2075.

Koeberl C. 1993. Chicxulub Crater, Yucatàn—Tektites, impact glasses, and the geochemistry of target rocks and breccias. *Geology* 21:211–214.

Koeberl C. and Sigurdsson H. 1992. Geochemistry of impact glasses from the K/T boundary in Haiti: Relation to smectites and a new type of glass. *Geochimica et Cosmochimica Acta* 56:2113–2129.

Koeberl C., Sharpton V. L., Schuraytz B. C., Shirey S. B., Blum J. D., and Marin L. E. 1994. Evidence for a meteoritic component in impact melt rock from the Chicxulub structure. *Geochimica et Cosmochimica Acta* 58:1679–1684.

Kring D. A. 1995. The dimensions of the Chicxulub impact crater and impact melt sheet. *Journal of Geophysical Research* 100:16979–16986.

Kring D. A. 1997. Composition of the earth's continental crust as inferred from the composition of impact melt sheets. 28th Lunar Planetary Science Conference. pp. 763–764.

Kring D. A. and Boynton W. V. 1991. Altered spherules of impact melt and associated relic glass from the K/T boundary sediments in Haiti. *Geochimica et Cosmochimica Acta* 55:1737–1742.

Kring D. A. and Boynton W. V. 1992. Petrogenesis of an augite-bearing melt rock in the Chicxulub structure and its relationship to K/T impact spherules in Haiti. *Nature* 358:141–144.

Kring D. A., Melosh H. J., and Hunten D. M. 1996. Impact induced perturbations of atmospheric sulfur. *Earth and Planetary Science Letters* 140:201–212.

Krogh T. E., Kamo S. L., Sharpton V. L., Marin L. E., and Hildebrand A. R. 1993. U-Pb ages of single shocked zircons linking distal K/T ejecta to the Chicxulub crater. *Nature* 366:731–734.

Lee W. J. and Wyllie P. J. 1996. Liquid immiscibility in the join $NaAlSi_3O_8$-$CaCO_3$ to 2.5 GPa and the origin of calciocarbonatite magmas. *Journal of Petrology* 37:1125–1152.

Lopez-Ramos E. 1975. Geological summary of the Yucatàn Peninsula. In *The ocean basins and margins, Vol. 3: The Gulf of Mexico and the Caribbean,* edited by Nairn A. E. M. and Stehli F. G. New York: Plenum. pp. 257–282.

Martinez I., Agrinier P., Schärer U., and Javoy M. 1994. A SEM-TEM and stable isotope study of carbonates from the Haughton impact crater, Canada. *Earth and Planetary Science Letters* 121: 559–574.

Martinez I., Deutsch A., Schärer U., Ildefonse P., Guyot F., and Agrinier P. 1995. Shock recovery experiments on dolomite and thermodynamical calculations of impact induced decarbonation. *Journal of Geophysical Research* 100:15465–15476.
Morgan J., Warner M., and The Chicxulub Working Group 1997. Size and morphology of the Chicxulub impact crater. *Nature* 390:472–476.
Morgan J. V., Warner M. R., and Grieve R. A. F. 2002. Geophysical constrains on the size and structure of the Chicxulub impact crater. In *Catastrophic events and mass extinctions: Impacts and beyond,* edited by Koerbel C. and MacLEod K. G. Boulder: Geological Society of America. Special Paper 356. pp. 39–46.
Moore K. R. and Wood B. J. 1998. The transition from carbonate to silicate melts in the CaO-MgO-SiO_2-CO_2 system. *Journal of Petrology* 39:1943–1951.
Ocampo A. C., Pope K. O., and Fischer A. G. 1996. Ejecta blanket deposits of the Chicuxlub crater from Albion Island, Belize. In *The Cretaceous-Tertiary event and other catastrophes in Earth history,* edited by Ryder G., Fastovski D., and Gartner S. Boulder: Geological Society of America. Special Paper 307. pp. 75–88.
Osinski G. and Spray J. G. 2001. Impact-generated carbonate melts: Evidence for the Haughton structure, Canada. *Earth and Planetary Science Letters* 194:17–29.
Pierazzo E. and Melosh H. J. 1999. Hydrocode modeling of Chicxulub as an oblique impact event. *Earth and Planetary Science Letters* 165:163–176.
Pierazzo E., Vickery A. M., and Melosh H. J. 1997. A re-evaluation of impact melt production. *Icarus* 127:408–423.
Pierrazo E., Kring D. A., and Melosh H. J. 1998. Hydrocode simulation of the Chicxulub impact event and the production of climatically relevant gases. *Journal of Geophysical Research* 103:28607–28625.
Pilkington M. and Hildebrand A. 2000. Three-dimentional magnetic imaging of the Chicxulub crater. *Journal of Geophysical Research* 105:23479–23491.
Pope K. O. 2002. Impact dust not the cause of the Cretaceous-Tertiary mass extinction. *Geology* 30:99–102.
Pope K. O., Baines K. H., Ocampo A. C., and Ivanov B. A. 1994. Impact winter and the Cretaceous-Tertiary extinctions: Results of a Chicxulub asteroid impact model. *Earth and Planetary Science Letters* 128:719–725.
Pope K. O., Baines K. H., Ocampo A. C., and Ivanov B. I. 1997. Energy, volatile production, and climate effects of the Chicxulub Cretaceous/Tertiary boundary impact. *Journal of Geophysical Research* 102:21645–21664.
Pope K. O., Ocampo A. C., Fischer A. G., Alvarez W., Fouke B. W., Webster C. L., Vega F. J., Smit J., Fritsche A. E., and Claeys P. 1999. Chicuxlub impact ejecta from Albion Island, Belize. *Earth and Planetary Science Letters* 170:351–364.
Pye E. G., Naldrett A. J., and Giblin P. E. 1984. *The geology and ore deposits of the Sudbury structure.* Ontario: Ontario Geological Survey. 603 p.
Roddy D. J., Schuster S. H., Rosenblatt M., Grant L. B., Hassig P. J., and Kreyenhagen K. N. 1987. Computer simulations of large asteroid impacts into oceanic and continental sites; Preliminary results on atmospheric, cratering, and ejecta dynamics. *International Journal of Impact Engineering* 5:525–541.
Schuraytz B. C., Sharpton V. L., and Marín L. E. 1994. Petrology of impact-melt rocks at the Chicxulub multiring basin, Yucatàn, Mexico. *Geology* 22:868–872.
Sharpton V. L., Dalrymple G. B., Marín L. E., Ryder G., Schuraytz B. C., and Urrutia J. 1992. New links between the Chicxulub impact structure and the Cretaceous/Tertiary boundary. *Nature* 359:819–821.
Sharpton V. L., Marín L. E., Carney J. L., Lee S., Ryder G., Schuraytz B. C., Sikora P., and Spudis P. D. 1996. A model of the Chicxulub impact basin based on evaluation of geophysical data, well logs and drill core samples. In *The Cretaceous-Tertiary event and other catastrophes in Earth history,* edited by Ryder G., Fastovski D., and Gartner S. Boulder: Geological Society of America. Special Paper 307. pp. 55–74.
Siebenschock M., Schmitt R. T., and Stöffler D. 1998. Suevite from Hohenaltheim: A new deposit from the Ries crater, Germany (abstract). 29th Lunar and Planetary Science Conference. pp. 1020–1021.
Sigurdsson H., D'hondt S., Arthur M. A., Bralower T. J., Zachos J. C., Van Fossen M., and Channell J. E. T. 1991. Glass from the Cretaceous-Tertiary boundary in Haiti. *Nature* 349:482–487.
Smit J., Montanari A., Swinburne N. H. M., Alvarez W., Hildebrand A. R., Margolis S. V., Claeys P., Lowrie W., and Asaro F. 1992. Tektite-bearing, deep-water clastic unit at the Cretaceous-Tertiary boundary in northeastern Mexico. *Geology* 20:99–103.
Stöffler D. 1977. Research drilling Nördlingen 1973: Polymict breccias, crater basement, and cratering model of the Ries impact structure. *Geologica Bavarica* 75:443–458.
Stöffler D. and Grieve R. A. F. 1994. Classification and nomenclature of impact metamorphic rocks: A proposal to the IUGS subcommission on the systematics of metamorphic rocks (abstract). 25th Lunar and Planetary Science Conference. pp. 1347–1348.
Stöffler D. and Langenhorst F. 1994. Shock metamorphism of quartz in nature and experiment: 1. Basic observation and theory. *Meteoritics* 29:155–181.
Stöffler D., Ewald U., Ostertag R., and Reimold W. U. 1977. Research drilling Nördlingen 1973 (Ries): Composition and texture of polymict impact breccias. *Geologica Bavarica* 75: 163–189.
Stöffler D., Knöll H. D., and Maerz U. 1979. Terrestrial and lunar impact breccias and the classification of lunar highland rocks. Proceedings, 10th Lunar and Planetary Science Conference. pp. 639–675.
Stöffler D., Deutsch A., Avermann M., Bischoff L., Brockmeyer P., Buhl D., Lakomy R., and Müller-Mohr V. 1994. The formation of the Sudbury Structure, Canada: Toward an unified impact model. In *Large meteorite impacts and plantary evolution,* edited by Dressler B. O., Grieve R. A. F., and Sharpton V. L. Boulder: Geological Society of America. Special Paper 293. pp. 303–318.
Swisher C. C., III, Grajales-Nishimura J. M., Montanari A., Margolis S. V., Claeys P., Alvarez W., Renne P., Cedillo-Pardo E., Maurrasse F. J. M. R., Curtis G. H., Smit J., and McWilliams M. O. 1992. Coeval $^{40}Ar/^{39}Ar$ ages of 65.0 million years ago from Chicxulub crater melt rock and Cretaceous-Tertiary boundary tektites. *Science* 257:954–958.
Ward W. C., Keller G., Stinnesbeck W., and Adatte T. 1995. Yucatàn subsurface stratigraphy: Implications and constraints for the Chicuxlub impact. *Geology* 23,873–876.
Warren P. H., Claeys P., and Cedillo-Pardo E. 1996. Mega-impact melt petrology (Chicxulub, Sudbury, and the Moon): Effects of scale and other factors on potential for fractional crystallization and development of cumulates. In *The Cretaceous-Tertiary boundary event and other catastrophes in Earth history,* edited by Ryder G., Fastovsky D., and Gartner S. Boulder: Geological Society of America. Special Paper 307. pp. 105–124.
Wyllie P. J. 1989. Origin of carbonatites; Evidence from phase equilibrium studies. In *Carbonatites: Genesis and evolution,* edited by Bell K. London: Unwin Hyman. pp. 500–545.
Yang W. B. and Ahrens T. J. 1998. Shock vaporization of anhydrite and global effects of the K/T bolide. *Earth and Planetary Science Letters* 156:125–140.